



Tuning inertial nonlinearity for passive nonlinear vibration control

Samuel C. Stanton · Dean Culver · Brian P. Mann

Received: 11 January 2019 / Accepted: 4 November 2019 / Published online: 21 November 2019
© US Government 2019

Abstract This paper examines the viability of completely passive control approach based on multiple timescale perturbation methods to elicit desired dynamic cancellation or suppression of nonlinear vibration characteristics. Without appeal to feedback, auxiliary oscillating systems, or nonlinear energy sinks, we demonstrate how inertial nonlinearity balancing can more simply realize distortion-free vibrational responses that are robust to very strong forcing amplitudes across resonant, super-harmonic, and sub-harmonic excitation frequencies as well as opportunities to passively suppress hysteresis, cusp-fold bifurcations, and higher harmonics. Of particular merit are the variegated results concerning critical design points for passive control of sub-harmonic resonances. To most simply capture the essence and broad relevance of the approach, we focus upon a variant of the Duffing oscillator that describes moderately large amplitude vibration of a cantilever beam, various link systems, and kinematically constrained particle motion. The results herein are anticipated to be the most relevant

to NEMS/MEMS-based sensing research and technology as well as vibration-based mechanical energy harvesting or mechanical filtering.

Keywords Inertial nonlinearity · Method of multiple scales · Passive vibration control · Mechanical filter

1 Introduction

Harmonics overlooked by linear dynamic models are often an unwanted result of system nonlinearity and, at worst, can be the cause of dangerous or damaging consequences. Much attention is given to such issues in electrical utilities, where the failure of many different components attached to the grid is stressed due to the presence of harmonics in the AC signals, perhaps generated by thyristors [1] or switch mode power supplies [2]. This includes, but is certainly not limited to, reduced lifetime of motors, failure in grid capacitors, and reduced delivery efficiency [3]. However, the challenges presented by harmonics in oscillating signals do not stop at the boundaries of electrical systems. Harmonics in mechanical systems and structures often cause unanticipated stresses (especially if the system experiences excitation matching its main resonance [4]), leading again to reduced lifetime if not outright failure.

In addition, such harmonics distort the signals generated by mechanical sensors, thus limiting their signal-to-noise ratios and effective bandwidth. Capturing the

S. C. Stanton (✉)
Engineering Sciences Directorate, US Army Research
Office, Adelphi, USA
e-mail: samuel.c.stanton2.civ@mail.mil

D. Culver
Vehicle Technology Directorate, US Army Research
Laboratory, Adelphi, USA

B. P. Mann
Mechanical Engineering and Material Science Department,
Duke University, Durham, USA

influence of higher harmonics becomes even more crucial in nanoscale and microscale structures [4], particularly in sensory application like piezoelectric micro-cantilevers in scanning force microscopes [5] where precision is the primary design metric. Moreover, such sensors are designed for extremely low quality factors, which increases the propensity for highly distorted motions due to sub-harmonic resonance.

Many investigators seek to eliminate non-negligible higher harmonics in structural vibration with active control techniques. A brief review of active control techniques in aeroelastic applications can be found in the work of Librescu and Marzocca [6], where the authors break down various approaches under the headings of Collar's triangle. Many more general techniques exist, such as the nonlinear modified positive position feedback (NMPPF) approach presented by Omid [4] or an incremental finite-element procedure from Gao [7]. For a thorough review of vibration isolation techniques applied to microscale systems, see the work of Liu et al. [8].

Active vibration control requires precise detection, costly computation, and challenging feedback schemes. A simpler and oftentimes more desirable approach is passive suppression or elimination of undesirable nonlinear behaviour. Suppressing higher harmonics with passive components has abundantly clear benefits in light of the design and fabrication hurdles that active methods require. One way that investigators and engineers have leveraged passive techniques to absorb vibrations is targeted energy transfer (TET), sometimes called nonlinear energy pumping [9, 10]. Born of the classic tuned vibration absorber (TVA) patented by Frahm, TET identifies design opportunities to create "vibration sinks" where vibrational energy will be localized [11] via geometric or component-wise control of elastic waves propagating in the system.

Here, we propose an alternative. By introducing additional discrete components in nonlinear systems featuring inertial and elastic nonlinearities, harmonics and various bifurcations that such systems may normally exhibit may be completely eliminated. Taking this approach elicits new opportunities for passive control of detrimental nonlinear vibration characteristics. While it is clear that balancing inertial and stiffness nonlinearities change the vibrational response of a nonlinear system, our results reveal non-intuitive sensitivities to the sign of both restoring force and inertial nonlinearities and especially subtle design points associ-

ated with sub-harmonic resonance. Moreover, to the best extent of the authors knowledge, a detailed exposition of the subtleties associated with passively cancelling sub-harmonic resonance does not exist. To date, all relevant studies are based on active feedback control or coupling to an auxiliary system (e.g. a tuned mass damper or nonlinear energy sink).

2 Passive control of nonlinear vibration characteristics

This paper considers a dimensionless form of a damped and driven Duffing oscillator that is augmented by nonlinear inertial forces

$$\ddot{x} + \beta(x^2\ddot{x} + x\dot{x}^2) + 2\mu\dot{x} + x + \alpha x^3 = \Gamma \cos(\Omega\tau). \quad (1)$$

This equation arises in a broad range of physics and engineering contexts for moderately large rotations and deflections. For example, Eq. (1) can be shown to describe the motion of kinematically constrained particles (e.g. motion along a parabolic path) [12], the vibration of systems comprised of interconnected links [13], and perhaps most importantly for the results in this paper: the moderately large amplitude motion of a cantilever beam's distinct vibration modes (spanning applications from aerospace lift-generating structures [14] to NEMS/MEMS sensors [15]). While this equation has been analysed to significant extent (especially in the structural dynamics literature), the intrinsic opportunity to modulate vibration characteristics due to the interplay between nonlinear inertial forces and nonlinear restoring forces has not been well explored. In the results that follow, our results are valid for the model in Eq. (1) that is premised on the third-order expansion of typical engineering systems experiencing moderately large deflections or rotations away from equilibrium. They are also limited to the validity of the multiple timescaling perturbation, where we presume the nonlinearities, damping, and forcing are of the same order. These are assessed to be reasonable presumptions for engineering systems.

2.1 Resonant cancellation and distortion-free nonlinear vibration

The results in this section are motivated by, and build upon, themes present in the distant and more recent lit-

erature. The primary purpose is to establish a framework for understanding the rationale and technical approach for the later results. In particular, we build upon foundations drawn from: (1) insight and comments in Ref [16] where perturbation methods indicate parameter settings where restoring force nonlinearities might have no effect, (2) numerical investigations by McHugh and Dowell [14] on offsetting nonlinearities in a physical system capable of being described by Eq. (1), and (3) a recent exposition on harmonic cancellation due to Culver et al. [17].

Equation (1) consists of only third-order nonlinearities that may be analytically approached by a perturbation solution with two timescales. Accordingly, real time τ is expressed as $T_m = \epsilon^m \tau$ for $m = 0, 1$ and a solution is assumed of the form $x(\tau; \epsilon) = x_0(T_0, T_1) + \epsilon x_1(T_0, T_1)$. In addition, we use shorthand for derivatives with respect to T_0 and T_1 as $d/d\tau = D_0 + \epsilon D_1$, and $d^2/d\tau^2 = D_0^2 + 2\epsilon D_0 D_1$, where $D_i = \partial/\partial T_i$. The nonlinear, damping, and forcing terms are set at order ϵ such that their effects will manifest in the solvability condition for moderate deflections and weak forcing. Upon substituting the perturbation of $x(\tau)$ and its subsequent time derivatives into the equation of motion, the following equations are obtained after collecting coefficients of ϵ^0

$$D_0^2 x_0 + x_0 = 0 \quad (2)$$

and for ϵ^1 :

$$D_0^2 x_1 + x_1 = -2D_0 D_1 q_0 - 2\mu D_0 x_0 - \alpha x_0^3 - \beta \left[x_0^2 D_0^2 x_0 + q_0 (D_0 x_0)^2 \right] + \Gamma \cos(\Omega \tau) \quad (3)$$

The first equation is a simple harmonic oscillator with a solution of the form $x_0 = A_1(T_1) \exp(i\Omega T_0) + \text{c.c.}$ where the amplitude $A_1(T_1)$ is a complex number and c.c. indicates complex conjugate of the first term. Substituting this solution into the right-hand side of Eq. (3) gives a series of harmonic forcing sources to the differential equation for x_1 .

Since the fundamental frequency of the system is nondimensionalized to one, we are interested in values for forcing frequency of $\Omega = 1$ for harmonic excitation, $\Omega = 3$ for sub-harmonic excitation, and $\Omega = 1/3$ for super-harmonic excitation. To concisely capture each of these cases in the perturbation analysis, we expand the excitation frequency as $\Omega = n + \epsilon\sigma$ where a detuning parameter $\sigma = \mathcal{O}(1)$ is introduced to express the nearness of the forcing to a frequency range of interest.

Substituting the forcing frequency expression into the perturbation equation gives

$$D_0^2 x_1 + x_1 = \left[2in(A' + \mu A) + (2n^2\beta - 3\alpha)A^2\bar{A} + \frac{1}{2}\Gamma e^{i\sigma T_1} \right] e^{inT_0} + (2n^2\beta - \alpha)A^3 e^{3inT_0} + \text{c.c.}, \quad (4)$$

where the terms on the right-hand side will be further investigated for resonant ($n = 1$), sub-harmonic ($n = 3$), and super-harmonic ($n = 1/3$) excitation.

Excitation near resonance will give the condition for eliminating secular terms in the solution to x_1 as

$$2i(\mu A + A') + (2\beta - 3\alpha)A^2\bar{A} - \frac{1}{2}\Gamma e^{i\sigma T_1} = 0 \quad (5)$$

Examining this equation indicates that for $\beta = 3\alpha/2$, the nonlinear effects due to restoring forces and inertial forces will cancel. Similar effects can be had for restoring forces alone in the presence of quadratic and cubic restoring forces as pointed out in Ref. [16]. We henceforth reference the dynamic cancellation effect as *resonant cancellation*.

Solving the amplitude-dependent frequency response function permits graphical illustration of the phenomenon. Presuming a complex form for the amplitudes of the form $A = a(T_1) \exp[i\theta(T_1)]/2$ with a phase expressed in terms of the frequency detuning as $\theta = \sigma T_1 - \phi$ accomplishes a transformation to a nonlinear algebraic frequency response function

$$a^2 \left(\mu^2 + \left[\frac{1}{8} (2\beta - 3\alpha) a + \sigma \right]^2 \right) = \frac{\Gamma^2}{4}, \quad (6)$$

where the critical tuning value is seen to be in direct proportion to higher-order amplitude values. At critical tuning, the usual linear frequency response function is recovered.

Solutions for the fully nonlinear algebraic amplitude equation were found by solving for σ for a range of amplitudes a with the results shown in Fig. 1. The cases illustrated are for $\alpha = 1$ and varying values of inertial nonlinearity. Balancing inertial nonlinearities against nonlinear restoring forces leads to a dynamic cancellation of hysteresis phenomenon and an associated natural elimination of cusp-fold bifurcations. A numerical exploration of almost complete dynamic cancellation of inertial versus stiffness nonlinearities in an inextensible cantilever beam is discussed in McHugh in Dowell [14]. A path towards achieving complete cancellation can be realized by attaching an appropriately sized

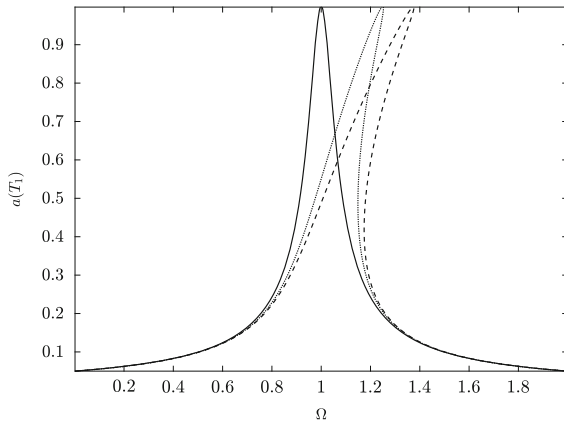


Fig. 1 Amplitude-dependent frequency response cancellation at resonance. The solid line is when β is tuned to the critical value of $3\alpha/2$ while the dotted and dashed lines are for when β is $\alpha/2$ and 0, respectively. Other parameters include $\alpha = 1$, $\mu = 0.05$, and $\Gamma = 0.1$

end mass. This result might benefit vibration-based sensing methodologies as well as enhancing vibration-based power generation when harvesting energy from a narrow-band source.

The perturbation solution reveals a second opportunity for passive vibration control as described in Culver et al [17] and henceforth referred to as *distortion-free nonlinear vibration*. Higher harmonic corrections to the first perturbation solution are available by solving higher-order ϵ equations. In particular, by solving Eq. (3) with secular terms eliminated, a parameter tuning opportunity is shown to exist such that the amplitudes proportional to various forcing terms in the perturbation solution are eliminated. This will be shown to be effective for resonant, super-harmonic, and sub-harmonic excitation. In Culver et al., a general framework is derived and illustrated in detail for the case of resonant excitation of an inextensible cantilever beam. Therein, the parameters for inertial and stiffness nonlinearity due to enforcing a holonomic inextensibility constraint alongside the convenient opportunity to passive tune through a concentrated end mass are detailed. For the model system in Eq. (1), the order ϵ perturbation equation with secular terms removed is of the form

$$D_0^2 x_1 + x_1 = (2\beta - \alpha) A^3 e^{3iT_0} + \text{c.c.}, \quad (7)$$

where for resonant excitation, we set $n = 1$. Inspecting the right-hand side indicates that higher harmonics will not be excited if the condition $\beta = \alpha/2$ is satis-

fied. Opting for this design point sacrifices control of resonant hysteresis phenomenon due to resonant cancellation as shown in Fig. 1. Instead, tuning to $\beta = \alpha/2$ creates an opportunity to eliminate signal distortion due to the emergence of higher harmonics. Figure 2 illustrates how nonlinear terms elicit rich harmonic content that completely disappears upon appropriately tuning the first higher harmonic correction term. However, various higher frequency anti-resonances, which could be of design interest for other vibration control objectives, are also sacrificed along the way. Further discussion on this case is available in Ref. [17], where β is also studied as a control parameter and the parameter range for β for resonant cancellation is shown to be extremely narrow.

2.2 Passive control of sub-harmonic and super-harmonic resonances

Earlier, it was remarked that the development around distortion-free nonlinear response was extensible beyond resonant excitation. However, all demonstrations so far have concerned forcing at the fundamental frequency (see also Ref. [17]). In this section, it is explicitly shown how the perturbation approach to distortion suppression can be derived for both sub-harmonic and super-harmonic excitation conditions.

For such non-resonant hard excitation, setting the excitation amplitude to order ϵ^0 is necessary. Modifying the perturbation equations accordingly yields the zeroth-order equation for ϵ to be

$$D_0^2 x_0 + x_0 = \Gamma \cos(\Omega\tau), \quad (8)$$

which has a solution of the form

$$x_0 = A(T_1)e^{iT_0} + \Lambda e^{i(nT_0 + \sigma T_1)} + \text{c.c.} \quad (9)$$

where

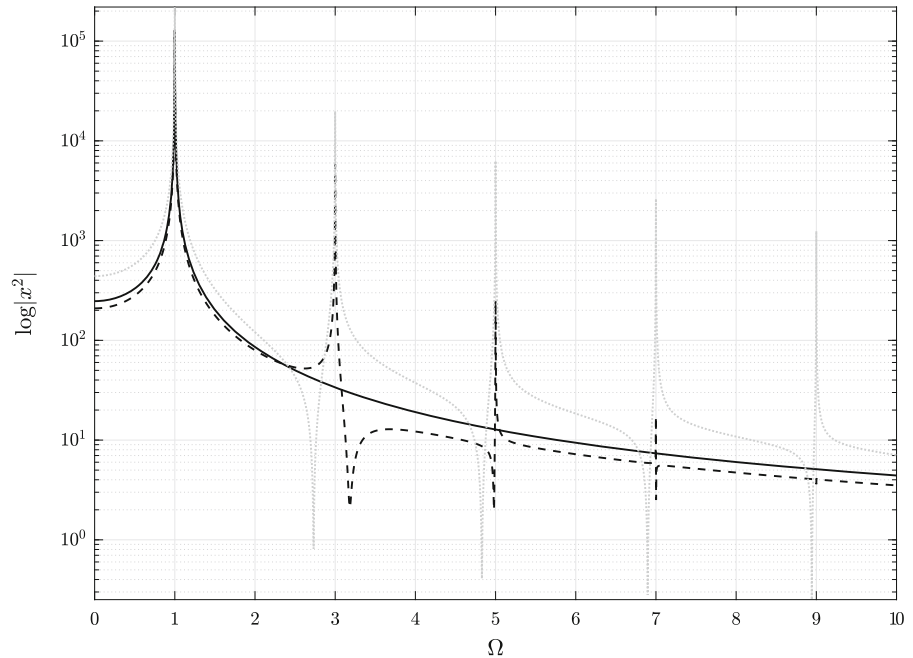
$$\Lambda = \frac{\Gamma}{2(1 - n^2)}. \quad (10)$$

This first-order solution is useful for both sub-harmonic and super-harmonic resonance studies. The third-order nonlinearities suggest a sub-harmonic resonance at $\Omega = 3$ and a super-harmonic resonance at $\Omega = 1/3$.

2.2.1 Sub-harmonic resonance

For lightly damped systems, typical of many NEMS/MEMS oscillator technologies, sub-harmonic resonance can be quite strong. However, tuning an inertial

Fig. 2 Eliminating distortion due to higher harmonics with $\beta = \alpha/2$ (solid line). For comparison, the power spectra for $\beta = 0$ (dashed line) and $\beta = 3\alpha/2$ (grey-dotted line) are shown. Other parameters include $\alpha = 1$, $\mu = 0.05$, and $\Gamma = 1$



nonlinearity can provide a robust mechanism for significantly suppressing this phenomenon. To quantitatively predict this behaviour, we begin by setting $n = 3$ in Eq. (4) to derive the following solvability condition for the growth of sub-harmonic amplitudes:

$$-2i(A' + \mu A) + 2(10\beta - 3\alpha)\Lambda^2 A + (2\beta - 3\alpha)A^2 \bar{A} + 3(2\beta - \alpha)\Lambda \bar{A}^2 e^{i\sigma T_1} = 0. \quad (11)$$

Steady-state solutions satisfying the solvability condition are found by using a complex exponential form for $A(T_1)$ in the same way as studied in the previous section with the exception that the phase is now $3\theta = \sigma T_1 - \phi$. The corresponding steady-state response is given by

$$\frac{\sigma}{3} + (10\beta - 3\alpha)\Lambda^2 + \frac{1}{8}(2\beta - 3\alpha)a^2 = -\frac{3}{4}(\alpha - 2\beta)\Lambda a \cos \phi, \quad (12)$$

$$-\mu = \frac{3}{4}(1 - 2\beta)\Lambda a \sin \phi. \quad (13)$$

Squaring and adding these equations to eliminate ϕ give the frequency response as the following nonlinear algebraic equation

$$\mu^2 + \frac{1}{9}[\sigma + p\Lambda^2 + qa^2]^2 = r\Lambda^2 a^2 \quad (14)$$

where $p = 3(10\beta - 3\alpha)$, $q = 3(2\beta - 3\alpha)/8$, and $r = 3(\alpha - 2\beta)/4$. Since this equation is quadratic in

a^2 , the solution is apparent and conditions for which the amplitudes are zero separates regions where there can be nontrivial solutions for the sub-harmonic response. This demarcation is governed by

$$\Lambda^2 = \frac{2qr}{3r^2(r^2 - 4pq)} \left(r\sigma + \sqrt{r^2\sigma^2 + 9\mu^2(r^2 - 4pq)} \right) \quad (15)$$

and is derived for the condition $a = 0$. Above and below this demarcation, there do not exist sub-harmonic resonances. However, sub-harmonic resonances also do not exist when the right-hand side is equal to zero. This is governed by the nature of the poles and zeroes. For combinations of α and β , the zeroes indicate that there can also be no sub-harmonic solutions for special values of $\beta = \alpha/2$ or $3\alpha/2$ while poles associated with $\beta = 3\alpha(21 \pm 4\sqrt{14})/62$ will lead to large regions where sub-harmonic resonance will persist. Analysis of these conditions for varying values of β reveals very different ranges where sub-harmonic suppression may be induced for either softening-type restoring forces ($\alpha < 0$) or hardening-type restoring forces ($\alpha > 0$) that also depend on the sign of β . These critical points will be discussed in more detail below.

Presuming a softening-type restoring force and a positive inertial nonlinearity, the region within the curve demarcated by Eq. (15) becomes suppressed. Figure 3 illustrates this phenomenon in the $\Gamma - \sigma$ plane

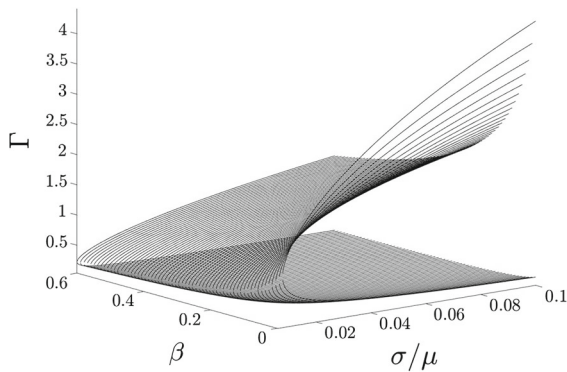


Fig. 3 Regions where nontrivial solutions may appear for varying values of β and σ when $\alpha < 0$. Other parameters include $\mu = 0.001$ and $\alpha = -1/6$. Nontrivial sub-harmonic resonance amplitudes occur inside the curve

while varying β . When $\beta = 0$, the region within the curve where nontrivial solutions can be seen to be substantially larger than when $\beta > 0$. Increasing the overall nonlinearity through larger β is seen to limit the region where sub-harmonic resonances can occur even as the amplitude of excitation is increased.

To test this prediction, a simulation was performed with the power spectrum results shown in Fig. 4. For a forcing amplitude of $\Gamma = 3$ and $\sigma = 0.15$, Eq. (15) predicts the response to lie in the nontrivial solution regime for the sub-harmonic amplitudes. Indeed, as the time series also makes clear, sub-harmonic resonance in this parameter regime has a strong effect on the frequency content and time series. The amplitudes are seen to be quite large in sub-harmonic resonance when inertial

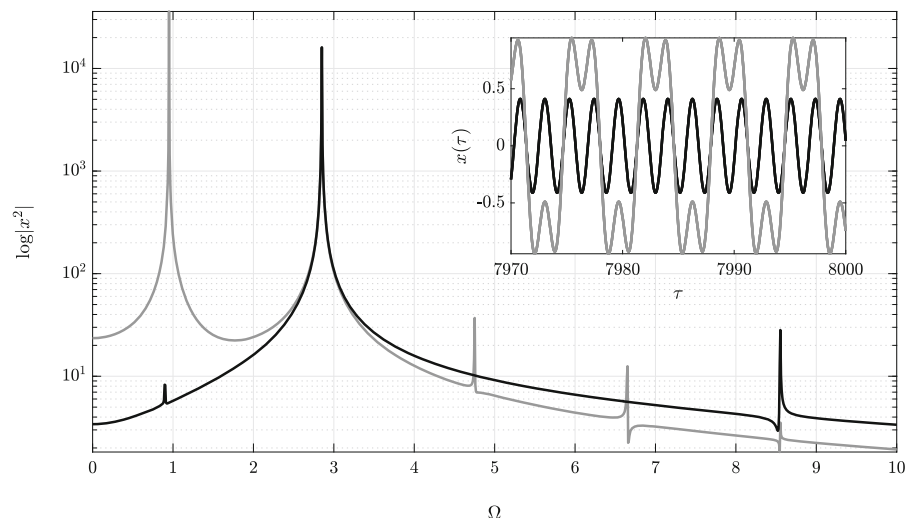
nonlinearities do not exist. However, a subtle increase to $\beta = 0.2$ is seen to nearly eliminate any remnants of the sub-harmonic effects. This is due to the suppression observed in Fig. 3. The same trend manifests from Eq. (15) when $\alpha > 0$ and $\beta < 0$.

The behaviour for a hardening-type restoring force ($\alpha > 0$) and a range of β , from negative to positive, is shown in Fig. 5. One can see the effect of various poles and zeros emanating from Eq. (15) to influence the region where nontrivial sub-harmonic amplitudes can exist (shaded grey areas). The zeros of $\beta = \alpha/2$ and $3\alpha/2$ lead to sub-harmonic suppression. Numerical values for the poles associated with $\beta = 3\alpha(21 \pm 4\sqrt{14})/62$ in Fig. 5 are given by $\beta = 0.04$ and 0.29 . For these values, the domain for sub-harmonic resonance is exceedingly robust and sub-harmonic resonance will persist for very large values of the forcing amplitude.

Guided by the insight provided by this figure, another simulation was performed for a region predicted to elicit large sub-harmonic resonance near a pole ($\beta = 0.05$) versus a domain associated with a the narrow zero $\beta = \alpha/2 = 1/12$. Figure 6 illustrates a profound impact of passively tuning to the zero predicted by Eq. (15). A more forgiving region is seen to be associated with the zero generated by $\beta = 3\alpha/2$. Increasing damping will reduce the grey regions in Fig. 5 and enlarge the narrow region around the pole.

Higher harmonics are more straightforward to eliminate. Substituting Eq. (2.2) into Eq. (3) (with external forcing now incorporated in the first perturbation equation) will give conditions for eliminating both resonant

Fig. 4 Suppressing sub-harmonic resonance for $\Gamma = 3$, $\mu = 0.001$, $\Omega = 2.85$, $\alpha = -1/6$, and $\beta = 0.2$ (solid black line). The power spectra for $\beta = 0$ (grey line, all other parameters the same) show a strong peak at $\Omega/3$ that is nearly eliminated by a subtle increase in inertial nonlinearity. Inset: corresponding time series data with suppressed resonance (black line) and no inertial nonlinearity (grey line)



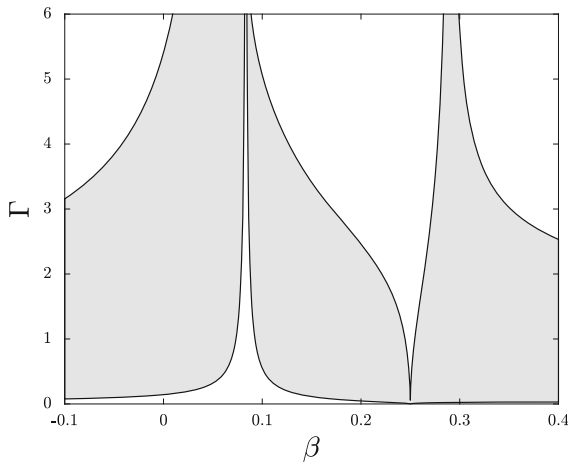


Fig. 5 Regions where nontrivial sub-harmonic resonance solutions can exist (grey shaded area) is strongly influenced by the poles and zeros of Eq. (15). The white space are regions where sub-harmonic resonance will be suppressed for $\alpha = 1/6$, $\sigma = 0.15$, and $\mu = 0.001$

excitation as well as higher harmonics. Since the next higher harmonic is 9Ω , all that is required to tune is to set the coefficient of terms in proportion to $\exp[9i T_0]$ to zero. The critical value for eliminating distortion during sub-harmonic excitation is revealed as $\beta = \alpha/18$. Figure 7 shows the robustness of the harmonic elimination effect even for a very strong forcing of $\Gamma = 10$. Again, eradicating the next higher harmonic suppresses the cascade of integer multiple harmonics as seen in the resonant case.

Realizing these results can be as straightforward as adjusting a tuning mass on a cantilever beam. Similarly, for a link-based system, this can be realized by modifying the centre of mass or the addition of a tuning mass as well. For constrained motion of a particle, modifying the characteristics of the constraint curve (e.g. the coefficients of the equations governing the constraint curve) will provide for very broad tunability of the inertial nonlinearity parameter. For cases in which the inertial properties cannot be varied, restoring force elements need to be modified.

2.2.2 Super-harmonic resonance

The case of super-harmonic resonance is for when $\Omega = 1/n$ and for the system under study $n = 3$. The super-harmonic resonance case requires similar reasoning for the secular terms as accomplished in the sub-harmonic resonance case. This is due to the fact that

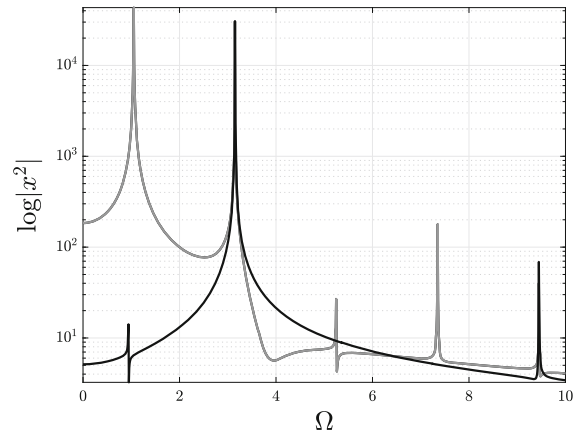


Fig. 6 Illustrations of the robustness of the sub-harmonic resonance despite a very large forcing amplitude $\Gamma = 7$ when properly tuned to a critical design point of $\beta = \alpha/2 = 1/12$ (black line). For comparison, the grey line is for when $\beta = 0.05$ and $\Gamma = 7$, a region predicted not to suppress sub-harmonic resonance. Other parameters include $\mu = 0.001$, $\Omega = 3.15$, and $\alpha = 1/6$

the next higher harmonic amplitude due to a $1/n$ excitation frequency is coincident with the term responsible for unbounded growth in the second-order perturbation equations. In this case, the solvability equation is

$$\begin{aligned} -2i(A' + \eta A) - \frac{9\Gamma^2}{128}(27\alpha - 10\beta)A \\ - (3\alpha - 2\beta)A\bar{A} + \frac{81\Gamma^3}{4096}(9\alpha - 2\beta) = 0. \end{aligned} \quad (16)$$

Further insight can be gained by developing the frequency response function in the same way as described for the resonant cancellation discussion. Substituting complex forms for $A(T_1)$ yields the following amplitude-dependent frequency response function for steady-state response amplitudes:

$$\begin{aligned} \left[\frac{9\Gamma^2}{256}(10\beta - 27\alpha) + \sigma + \frac{1}{4} \left(-\frac{3\alpha}{2} + \beta \right) a^2 \right]^2 a^2 \\ = \left[\frac{81\Gamma^3}{4096}(9\alpha - 2\beta) \right]^2. \end{aligned} \quad (17)$$

Upon dividing by the left-hand side term in brackets, Eq. (17) indicates that the numerator of the frequency response function will be zero when $\beta = 9\alpha/2$. Naturally, when the numerator vanishes there is no possibility of motion. Indeed, as depicted in Fig. 8 this condition will lead to distortion-free vibrational response in a manner as similarly robust as in the sub-harmonic case. Cancelling the harmonic associated with $3/n$ will

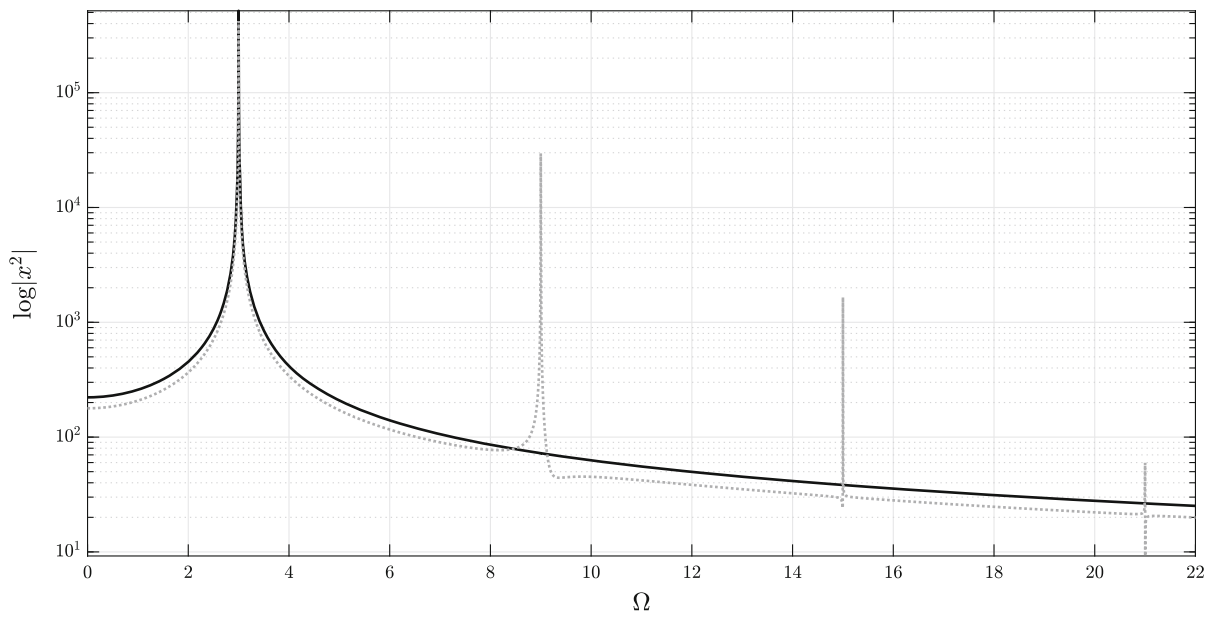


Fig. 7 Eliminating harmonic distortion during sub-harmonic resonance for $\Gamma = 10$, $\mu = 0.05$, $\Omega = 3$, $\alpha = 1$, and β tuned to the suggested design point of $\alpha/18$ (black line). For comparison,

the power spectra for $\beta = 0$ at the same excitation amplitude and frequency are shown by the grey-dotted line

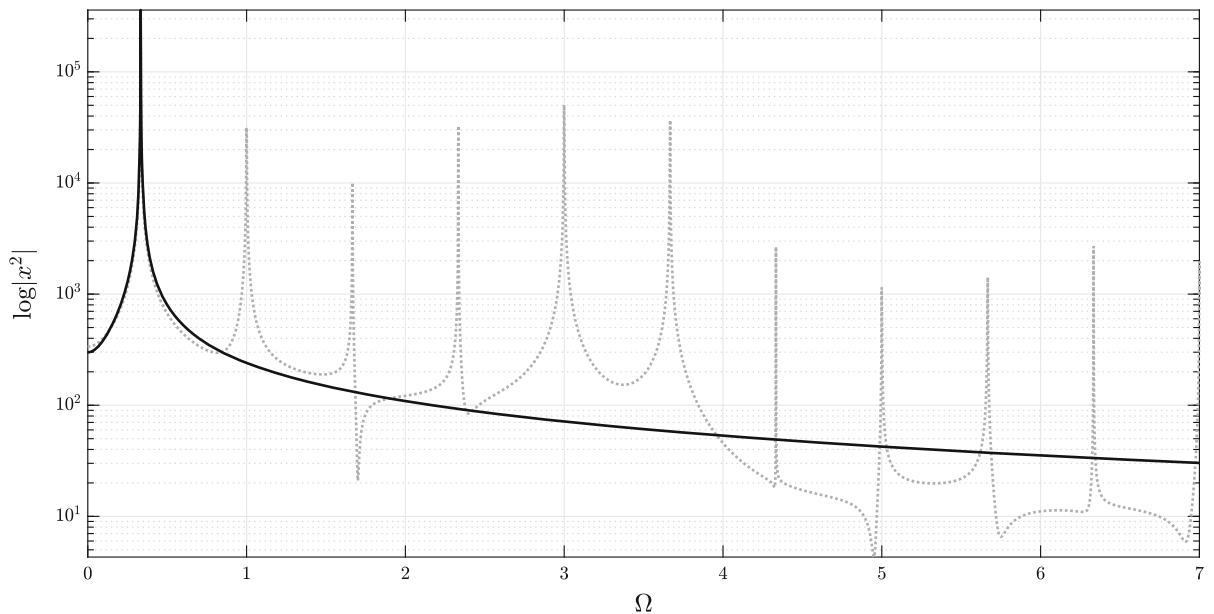


Fig. 8 Eliminating harmonic distortion during super-harmonic resonance for $\Gamma = 10$, $\mu = 0.05$, $\Omega = 1/3$, and β tuned to the suggested design point of $9\alpha/2$ (black line). For comparison, the

power spectra for $\beta = 0$ at the same excitation amplitude and frequency are shown by the grey-dotted line

lead to a cascade of higher harmonic amplitude cancellation.

3 Conclusion

Harmonic distortion is often an unwanted consequence of system nonlinearity. This paper investigated a passive control or tuning strategy for annihilating various types nonlinear effects. More specifically, perturbation analyses were used to demonstrate parameter combinations for inertial and restoring force nonlinearities that will alleviate a hardening-type response near primary resonance and also eliminate higher harmonics in the system's response. An important finding from these investigations was that specific expressions could be obtained for the parameter ratios, relationships between the inertial and restoring force parameters that can annihilate the nonlinear effects.

This paper additionally investigated tuning the inertial and restoring forces to eliminate sub- and super-harmonic resonances. Similar to the other examples studied, these cases also provided insightful relationships between the inertial and restoring force parameters. In particular, these relationships unveiled parameter combinations that will eliminate the sub- and super-harmonic resonances.

This paper considered a dimensionless form of a damped and driven Duffing oscillator with nonlinear inertial forces. Perturbation analyses were used to obtain expressions that related the response behaviour to the physical parameters of the system. This allowed specific relationships to be derived that enable the system's inertial and restoring force nonlinearities to offset one another and thus potentially eliminate the types of response behaviour investigated by the perturbation analysis. Although the present study focuses on a specific example, the authors believe the approach taken here is broadly applicable to the engineering community and that a similar approach could be taken to eliminate unwanted nonlinear response behaviour in many other engineered systems.

Acknowledgements The views expressed are those of the writer and not the Army, DoD, or its components. This material is based upon work supported by, or in part by, the U. S. Army Research Laboratory and the U. S. Army Research Office under contract/Grant Number W911NF-12-R-0012-04.

Compliance with ethical standards

Conflict of interest The authors declare that they have no conflict of interest.

Human and animal rights No animals or human subjects were used during the course of the research.

References

1. Wang, X., Xu, L., Fu, P., Li, J., Wu, Y.: Harmonics analysis of the iter poloidal field converter based on a piecewise method. *Plasma Sci. Technol.* **19**, 1–8 (2017)
2. Xu, X., Collin, A., Djokic, S., et al.: Operating cycle performance, lost periodicity, and waveform distortion of switch-mode power supplies. *IEEE Trans. Instrum. Meas.* **67**, 2434–2443 (2018)
3. Singh, G.: Power systems harmonics research: a study. *Eur. Trans. Electr. Power* **19**, 151–172 (2009)
4. Omid, E., Mahmoodi, S.: Nonlinear vibration suppression of flexible structures using nonlinear modified positive position feedback approach. *Nonlinear Dyn.* **79**, 835–849 (2015)
5. Jalili, M., Dadfarnia, D., Dawson, D.: A fresh insight into the microcantilever-sample interaction problem in non-contact atomic force microscopy. *J. Dyn. Syst. Meas. Control* **126**, 327–335 (2004)
6. Librescu, L., Marzocca, P.: Advances in the linear/nonlinear control of aeroelastic structural systems. *Acta Mech.* **178**, 147–186 (2005)
7. Gao, J., Shen, Y.: Active control of geometrically nonlinear transient vibration of composite plates with piezoelectric actuators. *J. Sound Vib.* **264**, 911–928 (2003)
8. Liu, C., Jing, X., Daley, S., Li, F.: Recent advances in micro-vibration isolation. *Mech. Syst. Signals Process.* **56–57**, 55–80 (2015)
9. Lee, Y., Vakakis, A., Bergman, L., McFarland, D., Kerschen, G., Nucera, F., Tsakirtzis, S., Panagopoulos, P.: Passive nonlinear targeted energy transfer and its applications to vibration absorption: a review. *Proc. IMechE* **222**, 77–134 (2008)
10. Pennisi, G., Mann, B., Naclerio, N., Stephan, C., Michon, G.: Design and experimental study of a nonlinear energy sink coupled to an electromagnetic energy harvester. *J. Sound Vib.* **437**, 340–357 (2018)
11. Gendelman, O., Manevitch, L., Vakakis, A., M'Closkey, R.: Energy pumping in nonlinear mechanical oscillators: Part i—dynamics of the underlying hamiltonian system. *J. Appl. Mech.* **68**, 34–41 (2001)
12. Marinca, V., Herianu, N.: Determination of periodic solutions for the motion of a particle on a rotating parabola by means of the optimal homotopy asymptotic method. *J. Sound Vib.* **329**, 1450–1459 (2010)
13. Bayat, M., Pakar, I., Cveticanin, L.: Nonlinear free vibration of systems with inertia and static type cubic nonlineari-

- ties: an analytical approach. *Mech. Mach. Theory* **77**, 50–58 (2014)
14. McHugh, K., Dowell, E.: Nonlinear responses of inextensible cantilever and free-free beams undergoing large deflections. *J. Appl. Mech.* **85**, 1–8 (2018)
 15. Villanueva, L.G., Karabalin, R.B., Matheny, M.H., Chi, D., Sader, J.E., Roukes, M.L.: Nonlinearity in nanomechanical cantilevers. *Phys. Rev. B* **87**, 024304 (2013)
 16. Nayfeh, A., Mook, D.: *Nonlinear Oscillations*, 2nd edn. Wiley, Hoboken (1978)
 17. Culver, D., Mann, B., Stanton, S.: Passive subharmonic elimination. *Appl. Phys. Lett.* **113**, 1–3 (2018)

Publisher's Note Springer Nature remains neutral with regard to jurisdictional claims in published maps and institutional affiliations.